Fluctuations in Fluid Invasion into Disordered Media

Martin Rost,[1] Lasse Laurson,[2] Martin Dubé,[3] and Mikko Alava[2]

[1]*Theoretische Biologie, IZMB, Universität Bonn, 53115 Bonn, Germany*
[2]*Laboratory of Physics, Helsinki University of Technology, P.L. 1100, 02105 HUT, Espoo, Finland*
[3]*CIPP, Université de Québec à Trois-Rivières, C.P. 500, Trois-Rivières, Québec, G9A 5H7 Canada*

(Received 2 May 2006; published 31 January 2007)

Interfaces moving in a disordered medium exhibit stochastic velocity fluctuations obeying universal scaling relations related to the presence or absence of conservation laws. For fluid invasion of porous media, we show that the fluctuations of the velocity are governed by a geometry-dependent length scale arising from fluid conservation. This result is compared to the statistics resulting from a nonequilibrium (depinning) transition between a moving interface and a stationary, pinned one.

DOI: 10.1103/PhysRevLett.98.054502 PACS numbers: 47.56.+r, 05.40.−a, 47.61.Jd, 68.35.Ct

The dynamics of interfaces, domain walls, and fronts in disordered systems has attracted tremendous attention not only because of practical applications but also for the general interest in the emerging equations of motion and scaling laws. The presence of randomness is felt through both frozen (or "quenched") noise and "thermal" fluctuations. Experimentally tested scenarios include fire fronts in combustible media [1], cracks propagating in solids [2–4], domain walls in magnets [5–9], and interfaces in multiphase flows ("imbibition" or "capillary rise" phenomena) [10–14], to name a few.

In these examples, the fluctuations of the fronts can generally be described via self-affine fractals, with dynamics exhibiting critical correlations. For time-independent randomness, such as the pore structure in fluid invasion, it is possible to concentrate on the zero-temperature phase transition which separates moving interfaces from pinned ones. The situation is then represented in terms of an order parameter, the velocity of the interface, and a control parameter, the driving force. The interface is described by a height $h(\mathbf{x}, t)$, at position $\mathbf{x} \in \mathbb{R}^d$ and time t, with its dynamics given by a Langevin equation $\partial_t h = \mathcal{L}(\{h\}, \alpha(\{h\}, \mathbf{x}, t))$. The kernel $\mathcal{L}$ contains the deterministic contribution of the interface and the random contribution of the noise configuration $\alpha(\{h\}, \mathbf{x}, t)$. Both may depend nonlocally on the entire interface configuration, denoted by $\{h\}$.

The scaling exponents of $h(\mathbf{x}, t)$ are often studied but are by no means the only interesting feature of this problem. It is also possible to study the amplitude of the various correlation functions, together with the persistence properties of the interface [15], or the scaling of probability distributions of quantities such as deviations of the interface from its average position or velocity.

Here we study the velocity fluctuations of driven fluid interfaces in disordered porous media in an imbibition situation, where a viscous fluid displaces air or a less viscous fluid. It is an important problem in the general field of fluid flow in porous media, with many engineering and technological applications. Fluid invasion and multiphase flows are often analyzed via lattice models of pore networks (e.g., for oil industry applications) or via "upscaling techniques," which summarize the physics on a coarse-grained (volume element) scale. One often studied aspect is the averaging of the scale-dependent permeability $\kappa(\mathbf{r})$, from the smallest pore scale up to geological scales [16–19]. It is not trivial to arrive at a coarse-grained description of these systems, since the physics is governed by the (conserved) fluid flow in the porous bulk coupled to microscopic interfaces—menisci—between the two fluids.

We report on the behavior of the spatially averaged interface velocity $v(t)$, directly related to the liquid intake under an externally controlled pressure. We first show that there exists a scaling relation between the velocity fluctuations Δv and the average velocity $\bar{v} = \langle v(t) \rangle$. This scaling is also reflected in the power spectrum of $v(t)$, as we discuss in detail. The scaling arguments are backed with numerical simulations of a phase-field model for imbibition [20]. We also study the interface velocity fluctuations for nonconserved, "local" dynamics, where we find a *different* scaling relation, again backed by simulations of the appropriate model [21]. Both the average flux as well as its fluctuations are experimentally well accessible, so our theoretical approach allows for an easy assessment of the type of dynamics. The detailed experiments of the Barcelona group and others point into that direction [10–14], and the main result extends to other systems where the front invasion depends on a conserved quantity.

The interface advances because fluid is transported from the reservoir through the medium. By Darcy's law, fluid flow is proportional to a pressure gradient:

$$\mathbf{j} = -\frac{\kappa}{\eta} \nabla P. \tag{1}$$

Here η is the viscosity of the liquid and κ the permeability of the medium. Deviations from Eq. (1) are known to arise for microscopic reasons, such as, e.g., inertial effects when a meniscus enters a pore, clogging by advected particles as in the case of a dye, and the partial wetting of capillaries.

Nevertheless, the linear form already leads to rich phenomena [22].

For an incompressible fluid, a Laplace equation $\nabla^2 P = 0$ governs the pressure field in the bulk. The appropriate boundary conditions are (i) $P \equiv P_R$ at the contact to a reservoir of liquid with constant pressure, and (ii) $P_I = \gamma^* \mathcal{K} + P_c + P_0$ at the interface. Condition (ii) is a superposition of atmospheric (P_0) and capillary (P_c) pressure on the pore scale and the effect of curvature $\mathcal{K}$ on a *coarse-grained* scale by an effective interface tension γ^*. For weak disorder, as arises in, e.g., paper, it is close to the bare value γ but may be much smaller in porous materials with weakly connected channels such as Vycor glass [23].

For $P_R = P_0$, imbibition is spontaneous with an average velocity $\bar{v} \equiv \partial_t \bar{h} = (\kappa/\eta) P_c/\bar{h}$, where $\bar{h}(t)$ is the average height. This leads to Washburn's law of capillary rise: $\bar{h} \sim t^{1/2}$ [24]. Forced imbibition arises by increasing the pressure at the reservoir as the interface advances. A constant mean pressure gradient $|\nabla P| = (P_R - P_I)/\bar{h} = \eta \bar{v}/\kappa$ keeps the average velocity $\bar{v}$ constant.

Quenched disorder in the porous structure roughens the interface around its average position. Capillary disorder $p_c(\mathbf{r}) = P_c + \delta p_c(\mathbf{r})$ acts only at the interface, and permeability disorder $\kappa(\mathbf{r}) = \kappa + \delta\kappa(\mathbf{r})$ controls the flux of liquid from the reservoir to the interface. If r_0 is the typical pore size and δr_0 its deviation, then $p_c \sim \gamma^*/r_0$ and $\kappa \sim r_0^2$, with $\delta p_c/\delta\kappa \sim p_c/\kappa$ [22,25].

Effective (capillary) interface tension and the average pressure gradient smoothen the interface and allow for correlated roughness only up to a lateral length scale

$$\xi_c \sim \sqrt{\frac{\kappa\gamma^*}{\eta\bar{v}}} = \sqrt{\frac{\kappa}{\mathrm{Ca}}} \tag{2}$$

related to the capillary number $\mathrm{Ca} = \eta\bar{v}/\gamma^*$ [20,22]. Its presence and dependence on $\bar{v}$ has also been confirmed experimentally [10,13]. The ratio of disorder strengths imposes another length scale

$$\xi_\kappa \sim \frac{\kappa^2}{\bar{v}\eta}\frac{\delta p_c}{\delta\kappa} = \frac{\sqrt{\kappa}}{\mathrm{Ca}} \tag{3}$$

separating regimes of different roughness. On scales shorter than ξ_κ, interface roughness is caused by capillary disorder and on larger scales by permeability disorder [22,25]. We consider the interesting case of a slowly advancing front, where $\xi_\kappa > \xi_c$, and capillarity-induced fluctuations prevail, and one has a well-defined interface [for stability, a Ca below $\sim\mathcal{O}(1)$ is needed [26]]. Then permeablity noise and its possible correlations with capillary disorder can be ignored.

The scaling behavior in imbibition can be demonstrated by model simulations [20]. A scalar phase field $\phi(\mathbf{r}, t)$ denotes by $\phi = 1$ the invaded (wet) and -1 the noninvaded (dry) regions, respectively. An energy functional

$$\mathcal{F}[\phi] = \int d^{d+1}r \left[\frac{(\nabla\phi)^2}{2} - \frac{\phi^2}{2} + \frac{\phi^4}{4} - \alpha(\mathbf{r})\phi\right] \tag{4}$$

couples the phase field to a space-dependent quenched randomness $\alpha(\mathbf{r})$, with average $\bar{\alpha}$ and standard deviation $\Delta\alpha$. This term models capillarity disorder, with the sign ($\alpha > 0$) favoring the wet phase $\phi = 1$. The model is defined on the half-space, $\mathbf{r} = (\mathbf{x}, y)$, with $y > 0$, with boundary conditions $\phi \equiv 1$ at $y = 0$ (coupled to a wet reservoir at the bottom) and the initial condition $\phi(\mathbf{r}, t = 0) \equiv -1$ (dry).

The corresponding chemical potential $\mu = \delta\mathcal{F}/\delta\phi$ (with the role of pressure in the context of imbibition) drives a current $\mathbf{j} = -\tilde{\kappa}\nabla\mu$ with a rescaled and possibly spatially varying mobility $\tilde{\kappa}(\mathbf{r})$. By local conservation of ϕ. this yields the dynamical equation

$$\partial_t\phi = -\nabla\cdot\tilde{\kappa}(\mathbf{r})\nabla[\nabla^2\phi + \phi - \phi^3 + \alpha(\mathbf{r})]. \tag{5}$$

With this model, a Young-Laplace relation between the chemical potential at the interface and the curvature $\mu_{\mathrm{int}} = \mathcal{K} - \alpha$ arises naturally.

The numerical simulations are performed, in a way that mimics forced-flow imbibition, by continuously shifting the fields $\phi(\mathbf{r}, t)$, $\tilde{\kappa}(\mathbf{r})$, and $\alpha(\mathbf{r})$ downward at velocity $\bar{v}$, as in the experiments of Ref. [27]. The stationary interface then has an average height $\bar{h} = \bar{\alpha}/(2\bar{v})$. For the Ca at hand, the permeability disorder has no influence (see [22]), nor have correlations between $\tilde{\kappa}(\mathbf{r})$ and $\alpha(\mathbf{r})$. Only simulations with capillary disorder are thus discussed here. Figure 1 shows examples of model interfaces in $d + 1 = 2$ dimensions, together with a time series of average velocity or liquid intake $v(t)$ exhibiting typical fluctuations. Figure 2 shows a spatiotemporal activity pattern of the local interface velocities $\partial_t h(x, t)$.

The *dynamics* of the roughening interface can be understood as a sequence of avalanches. At any given time, only a small localized portion of the interface is moving fast. There the Laplacian pressure field drags liquid from a surrounding region of *lateral* size $\bar{h}^d$, a region which therefore remains pinned. Farther away, the interface is not affected and moves independently. Within this region, the moving part has *maximal* capillary forces p_c. However, it eventually encounters disorder with lower p_c and gets

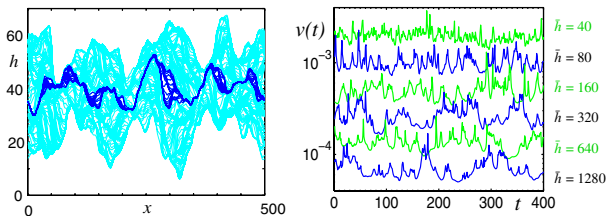

FIG. 1 (color online). Left: Interfaces $h(x, t)$ in a system of width $L = 500$ and average separation $\bar{h} = 320$ from the reservoir. The configurations are separated by time intervals $\Delta t = 500$ at 240 different times. Interface propagation is made visible by adding the constant shift velocity $\bar{v}$. The sequence of 20 black interfaces shows pinned and moving regions. Right: Time series of $v(t)$, the velocity for $L = \bar{h} = 40, 80, 160, \ldots, 1280$ from top to bottom, logarithmic scale in $v(t)$.

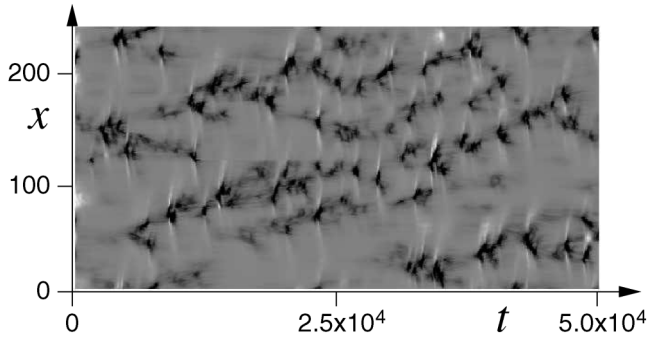

FIG. 2. Activity pattern in space (vertical) and time (horizontal). $L = 256$, $\bar{h} = 160$, lateral periodic boundary conditions. High velocities are dark, low velocities are light, and gray scale is nonlinear for better visibility. At any given time, activity is restricted to $n = L/\bar{h} \approx 2$ narrow avalanches of width ξ_c.

pinned. At this point, another region elsewhere starts to move. Propagation by avalanches in imbibition and their size distribution with one fixed scale has been found and discussed in experiments [14]. It is visible in Figs. 1 and 2. The size of these moving avalanches is given by the cutoff length scale $\xi = \xi_c$ or ξ_κ. The regime governed by capillary disorder has global roughness exponents $\chi \approx 1.25$ and a different local exponent $\chi_{\rm loc} = 1$ in $d + 1 = 2$ dimensions [20,22,28]. For higher Ca than those considered here, permeability disorder starts to play a role, and the exponents are $\chi = \chi_{\rm loc} = 1$ in $d + 1 = 2$ dimensions [22,25].

A key feature is the relation between an avalanche of duration τ and its volume $s(\tau)$. In general, a scaling $s(\tau) \sim \tau^\gamma$ may be expected, with the exponent γ determined as follows. Consider a region of lateral size ℓ swept over by an avalanche. Its vertical extent is related to ℓ by the *local* roughness exponent $w \sim \ell^{\chi_{\rm loc}}$ [20,28], with volume $s \sim \ell^{d+\chi_{\rm loc}}$. The avalanche is driven by a higher capillary pressure in the moving region as compared to other parts of the front. Since locally the values of p_c are independent random quantities, the excess driving force (the difference of typical p_c and the large fluctuation) and velocity decrease with size as $v \sim \ell^{-d/2}$. Therefore, the avalanche sweeping time scales as $\tau = w/v \sim \ell^{\chi_{\rm loc}+d/2}$ and leads to the relation $s \sim \tau^\gamma$, with

$$\gamma = \frac{\chi_{\rm loc} + d}{\chi_{\rm loc} + d/2}. \tag{6}$$

For $d = 1$, we have $\chi_{\rm loc} = 1$ [20] and expect $\gamma = 4/3$. In $d = 2$, we would expect using $\chi_{\rm loc} = \chi = 3/4$ [29] that $\gamma = 11/7$.

To see the scaling of velocity fluctuations Δv, we first relate the average avalanche velocity $\bar{v}_{\rm ava}$ to the overall velocity $\bar{v}$ by the relative size of moving parts $\bar{v}_{\rm ava} \approx (\bar{h}/\xi)^d \bar{v}$. Next we assume a simple relation $\Delta v_{\rm ava} \sim \bar{v}_{\rm ava}$ between the average avalanche velocity and its fluctuations, justified by the slow, intermittent motion. Thus,

$$\Delta v \approx \left(\frac{\bar{h}}{L}\right)^{d/2} \left(\frac{\xi}{\bar{h}}\right)^d \Delta v_{\rm ava} \tag{7}$$

by factors resulting from independence on scales larger than $\bar{h}$ and the relative fraction of moving parts on smaller scales. The relation between average avalanche velocity and fluctuations yields, in general, for both spontaneous and forced imbibition

$$\Delta v \sim \left(\frac{\bar{h}}{L}\right)^{d/2} \left(\frac{\xi}{\bar{h}}\right)^d \bar{v}_{\rm ava} \sim \left(\frac{\bar{h}}{L}\right)^{d/2} \bar{v}. \tag{8}$$

In spontaneous imbibition with rising height, $\bar{v} \sim 1/\bar{h}$ and $\Delta v \sim \bar{v}^{1-d/2} L^{-d/2}$. Equation (8) thus predicts that the fluctuations depend on the geometry (via $\bar{h}$ and L) and on the average velocity.

In the left panel in Fig. 3, we show the distributions of $P[v(t)]$ obtained in phase-field simulations for several values of $\bar{v}$ and *constant* square aspect ratio $L = \bar{h}$: They can be scaled by an ansatz $P(v) = \frac{1}{\bar{v}} \mathcal{P}(\frac{v-\bar{v}}{\bar{v}})$. The shape of $P[v(t)]$ resembles a Gumbel distribution of extreme value statistics reflecting avalanches in regions of maximal capillary pressure, but our data are too scarce for a careful analysis.

The avalanche motion is reflected in the power spectrum of the interface velocity $S(\omega) = \langle |\hat{v}(\omega)|^2 \rangle \sim \omega^{-\alpha}$. The exponent α may equal the exponent γ discussed previously, if the avalanches have a self-affine fractal spatiotemporal structure [30]. The right panel in Fig. 3 compares the power spectrum $S(\omega) = \langle |\hat{v}(\omega)|^2 \rangle$ of the mean interface velocity (solid line) to the average size $s(\tau)$ of avalanches with duration τ (dashed line). Both follow power laws $\omega^{-\alpha}$ and τ^γ, with $\alpha = \gamma \approx 4/3$, as predicted by Eq. (6).

The left panel in Fig. 4 shows Δv vs $\bar{v}$ for two different choices of the system geometry: $\bar{h}$ varying, with L fixed and with $L = \bar{h}$. We observe $\Delta v \propto \bar{v}^a$, with $a = 1$ for a square shape and $a = 1/2$ for fixed width, in agreement with our scaling picture. We checked also that for $L \gg \bar{h}$ the distribution $P[v(t)]$ gets sharper with increasing L, in agreement with the implication of the central limit theorem for independent random variables $\Delta v \sim L^{-1/2}$ [Eq. (8)].

An interface driven by a force F in a random medium *without* any conservation law obeys different scaling. In

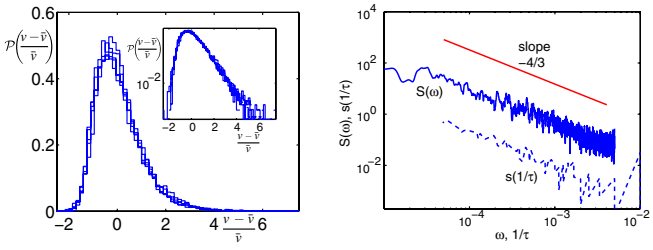

FIG. 3 (color online). Left: Rescaled distributions $\mathcal{P}(\frac{v(t)-\bar{v}}{\bar{v}})$ for various values of $1/\bar{v} \propto \bar{h} = L = 40, \ldots, 1280$. Right: Power spectrum $S(\omega) = \langle |\hat{v}(\omega)|^2 \rangle \propto \omega^{-4/3}$ for $\bar{h} = L = 1280$. The same exponent relates average avalanche size s and duration τ.

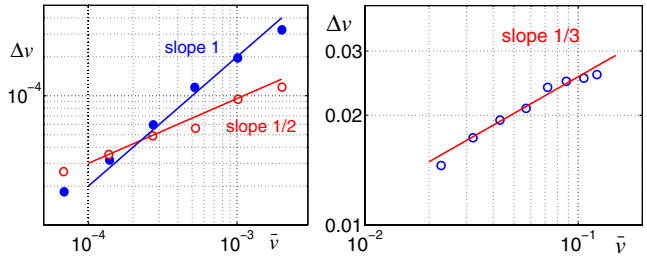

FIG. 4 (color online). Left: Fluctuations Δv vs mean $\bar{v}$ for constant width $L \equiv 500$ (open circles) and $L = \bar{h}$ (solid circles) follows $\Delta v \sim \bar{v}^a$ with $a = 1/2$ and 1, respectively; cf. Eq. (8). Lines with slope $1/2$ and 1, respectively, are to guide the eye. Right: The same for the local model of Ref. [21], with system size $L = 10^4$. The line has slope $1/3$.

the presence of a critical (zero-temperature, neglecting thermal creep) value F_c separating pinned and unpinned propagation, a correlation length $\xi \sim \Delta F^{-\nu}$ ensues, where $\Delta F = F - F_c$ and ν is the correlation length exponent. Meanwhile, the order parameter follows the generic scaling $\bar{v} \sim \Delta F^{\theta}$. In the critical region, when ΔF is so small that $\xi \approx L$, the order parameter exponent θ takes a nontrivial value smaller than unity. For slightly larger driving forces, we have $L > \xi$. In the simulations here, we considered $L/\xi = O(10)$, so we have $\bar{v} \sim \Delta F$ or a trivial effective $\theta_{\text{eff}} = 1$.

In a system of lateral size L, there are $N = (L/\xi)^d$ independent subvolumes. Inside these, the fluctuating locally averaged velocities v_i^{loc} are independent random variables with mean $\bar{v}$ and variance $\delta v^2 \sim \bar{v}^2$. Their average, the instantaneous velocity $v(t) = \sum_i v_i^{\text{loc}}/N$, then has fluctuations measured by

$$\Delta v \sim \delta v/\sqrt{N} \sim \bar{v}^{1-d\nu/(2\theta)}/\sqrt{L^d}. \tag{9}$$

Numerical simulations are performed with a cellular automaton for the quenched Edwards-Wilkinson equation [21] $\partial h/\partial t = \Gamma \nabla^2 h + F + \eta(x, h(x,t))$, where η is a quenched noise term with a bare correlator $\langle \eta(\mathbf{r})\eta(\mathbf{r}')\rangle = D\delta(\mathbf{r} - \mathbf{r}')$, with strength D. Γ is a surface tension similar to γ^*. The data are presented in the right panel in Fig. 4. They fit reasonably to the scaling ansatz of Eq. (9) with $1 - d\nu/(2\theta_{\text{eff}}) = 1/3$, derived from the known critical value $\nu \approx 4/3$ of the one-dimensional depinning transition [21] and $\theta_{\text{eff}} = 1$.

To summarize, we have presented a scaling theory for interface velocity fluctuations. Without detailed measurements of interface configurations but by the easily accessible fluctuations of the *average* interface propagation, one obtains information about the universality class of the process. Our arguments show the difference between dynamics with and without a bulk conservation law behind the interface. This is also manifest in the power spectrum of $v(t)$, where the avalanchelike dynamics allows one to understand the ensuing $1/f$ noise. The main argument applies to any dimensionality and is not dependent on the detailed model. A similar reasoning should extend to other systems where the global conservation of a quantity is important. One experimental possibility is vortex penetration dynamics in (high-T_c) superconductors—for which there is no known coarse-grained description [31,32]—since the vortex density is conserved.

This work has been supported by Deutsche Forschungsgemeinschaft and the Academy of Finland. We thank Lorentz Centre (Leiden, The Netherlands) and NORDITA (Copenhagen, Denmark) for kind hospitality.

[1] J. Maunuksela *et al.*, Phys. Rev. Lett. **79**, 1515 (1997).
[2] K. J. Måløy *et al.*, Phys. Rev. Lett. **96**, 045501 (2006).
[3] L. I. Salminen *et al.*, Europhys. Lett. **73**, 55 (2006).
[4] F. Kun *et al.*, Phys. Rev. Lett. **93**, 227204 (2004).
[5] L. V. Meisel and P. J. Cote, Phys. Rev. B **46**, 10 822 (1992).
[6] S. Hébert *et al.*, J. Solid State Chem. **165**, 6 (2002).
[7] V. Hardy *et al.*, Phys. Rev. B **70**, 104423 (2004).
[8] G. Durin and S. Zapperi, J. Stat. Mech. (2006) P01002.
[9] P. Paruch, T. Giamarchi, and J.-M. Triscone, Phys. Rev. Lett. **94**, 197601 (2005).
[10] D. Geromichalos, F. Mugele, and S. Herminghaus, Phys. Rev. Lett. **89**, 104503 (2002).
[11] J. Soriano *et al.*, Phys. Rev. Lett. **89**, 026102 (2002).
[12] J. Soriano *et al.*, Phys. Rev. Lett. **95**, 104501 (2005).
[13] J. Soriano, J. Ortín, and A. Hernández-Machado, Phys. Rev. E **66**, 031603 (2002); **67**, 056308 (2003).
[14] A. Dougherty and N. Carle, Phys. Rev. E **58**, 2889 (1998); R. Albert *et al.*, Phys. Rev. Lett. **81**, 2926 (1998).
[15] J. Merikoski *et al.*, Phys. Rev. Lett. **90**, 024501 (2003).
[16] B. Nœtinger, V. Artus, and Gh. Zargar, Hydrogeology J. **13**, 184 (2005); B. Nœtinger and Gh. Zargar, Oil Gas Sci. Technol. **59**, 119 (2004).
[17] A. Ahmadi and M. Quintard, J. Hydrol. **183**, 69 (1996).
[18] S. E. Gasda and M. A. Celia, Adv. Water Resour. **28**, 493 (2005).
[19] C. Braun, R. Helmig, and S. Manthey, J. Contam. Hydrol. **76**, 47 (2005); F. Cherblanc, M. Quintard, and S. Whitaker, Water Resour. Res. **39**, 1154 (2003).
[20] M. Dubé *et al.*, Phys. Rev. Lett. **83**, 1628 (1999).
[21] H. Leschhorn, Physica (Amsterdam) **195A**, 324 (1993).
[22] M. Alava, M. Dubé, and M. Rost, Adv. Phys. **53**, 83 (2004).
[23] P. Huber *et al.*, Europhys. Lett. **65**, 351 (2004).
[24] E. W. Washburn, Phys. Rev. **17**, 273 (1921).
[25] E. Pauné and J. Casademunt, Phys. Rev. Lett. **90**, 144504 (2003).
[26] R. Lenormand, J. Phys. C **2**, SA79 (1990).
[27] V. K. Horváth and H. E. Stanley, Phys. Rev. E **52**, 5166 (1995).
[28] J. M. López, M. A. Rodríguez, and R. Cuerno, Phys. Rev. E **56**, 3993 (1997).
[29] M. Dubé *et al.* (to be published).
[30] L. Laurson, M. Alava, and S. Zapperi, J. Stat. Mech. (2005) L11001.
[31] S. Zapperi, A. A. Moreira, and J. S. Andrade, Jr., Phys. Rev. Lett. **86**, 3622 (2001).
[32] E. Altshuler and T. H. Johansen, Rev. Mod. Phys. **76**, 471 (2004).